Optical flip-flop memory based on ring lasers sharing one active element with feedback through an extended cavity

Document status and date:
Published: 01/01/2004

Document Version:
Publisher's PDF, also known as Version of Record (includes final page, issue and volume numbers)

Please check the document version of this publication:

• A submitted manuscript is the version of the article upon submission and before peer-review. There can be important differences between the submitted version and the official published version of record. People interested in the research are advised to contact the author for the final version of the publication, or visit the DOI to the publisher's website.
• The final author version and the galley proof are versions of the publication after peer review.
• The final published version features the final layout of the paper including the volume, issue and page numbers.
Link to publication

Download date: 16. Nov. 2023

Ring-Laser Optical Flip–Flop Memory With Single Active Element

Shaoxian Zhang, Yong Liu, Daan Lenstra, Martin T. Hill, Heongkyu Ju, Giok-Djan Khoe, *Fellow, IEEE*, and H. J. S. Dorren

Abstract—We present a novel optical flip–flop configuration that consists of two unidirectional ring lasers with separate cavities but sharing the same active element unidirectionally. We show that in such a configuration light in the lasing cavity can suppress lasing in the other cavity so that this system forms an optical bistable element. Essential for obtaining the bistability is the presence of an additional feedback circuit that is shared by both lasers. We show experimentally that the flip–flop can be optically set and reset, has a contrast ratio of 40 dB and allows low optical power operation. We also present a model based on roundtrip equations. Good agreement between theory and experiments is obtained.

Index Terms—Flip–flop, memories, optical bistability, optical feedback, ring laser, semiconductor optical amplifiers, wavelength.

I. INTRODUCTION

OPTICAL flip–flop memories form key components in all-optical packet switches [1]. In order to employ optical flip–flop memories in telecommunication systems, the optical memories should allow a high switching speed, have a sufficiently high contrast ratio, and operate at low power. Reference [2] presents several well-known principles of optical bistability that can be applied in optical flip–flop memories. Examples of optical flip–flop memories that might be useful for futuristic telecommunication systems are presented in [3]–[9]. An interesting optical flip–flop memory based on two coupled lasers was presented in [7]. Essential in this flip–flop concept is that each laser has its own active element. Both lasers are symmetrically coupled to each other, and it was shown that in this configuration, the lasing light of one of the lasers can be used to suppress lasing of the other laser, so that the system acts as a master–slave configuration. It was shown the memory can be all-optically set and reset by low power optical pulses and operates with high contrast ratio of 40 dB. This configuration also turned out to be a useful concept in telecommunications technology since this optical flip–flop concept was used in optical packet switches and buffers [10]. The notion that symmetrically coupling of two nonlinear optical elements could lead to bistability and, thus,

flip–flop operation was further developed by showing that similar functionalities could be realized by symmetrically coupling of two Mach–Zehnder interferometers or nonlinear polarization switches [8], [9].

In this paper, we present a novel flip–flop concept that has essentially a contrast ratio as high as in [7], but it has one active element only. This flip–flop configuration consists of two unidirectional ring lasers with separate cavities but sharing the same active element unidirectionally. Each laser operates at a different wavelength. Essential for obtaining bistability in this system is that the lasing light output from the active element is partly fed back into the active element in the counterpropagating direction by an external cavity. We will show that such a configuration forms an optical bistable element and that switching between the states can be realized by injection of external light at the wavelength of the cavity that is not lasing. We will also show that we can obtain a contrast ratio of 40 dB between the states and that flip–flop operation can be realized by external light injection at low power.

We present a model that shows that the lasing light that is fed back via the extended cavity makes that if the roundtrip condition in one of the cavities can be satisfied. This explanation is supported by numerical simulation results that are in good agreement with experimental results.

The flip–flop configuration presented in this paper offers a number of advantages over alternative technologies. First of all, this flip–flop concept contains only one active element, which makes the configuration simple. Also, this concept can be monolithically integrated, which is persistent to successful utilization [11], [12]. A very important advantage is that this concept can be extended to a multistable system so that larger amounts of optical data bits can be stored. Furthermore, the bistability takes place over a large wavelength range, the concept is not tight to a specific technology and allows simple control over the threshold levels, it provides a large contrast range, and the flip–flop function can be all-optically set and reset with low power optical pulses.

The paper is organized as follows. In Section II, we present a model that describes the bistability as well as the switching operation. In Section III, we present the experimental results, which are well in agreement with the modeling results. Finally, the paper is concluded in Section IV.

II. OPERATION PRINCIPLE

Fig. 1 shows a schematic representation of the ring laser configuration with feedback. The roundtrip time equations for this system are derived in Appendix A. We have formulated the
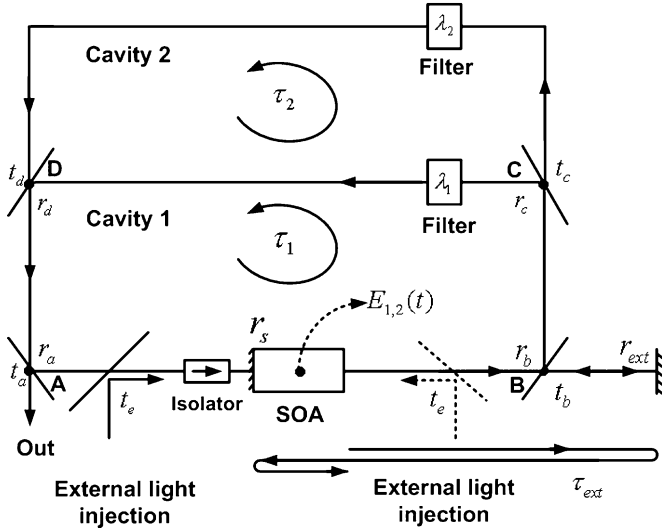
Fig. 1. Schematic of the flip–flop configuration. SOA: semiconductor optical amplifier.

dynamics of this system in terms of roundtrip time equations instead of rate equations, since, in the experimental implementation of this system, the lasers are composed out of discrete commercially available fiber pigtailed elements and, hence, each laser has a very large ring cavity length ($\sim$ 10 m). This means that the roundtrip times of the lasers are large compared to the carrier lifetime. The roundtrip equations for the fields are formulated at a reference point inside the semiconductor optical amplifier (SOA), as indicated in Fig. 1. The SOA itself is modeled as a point amplifier

$$
\begin{aligned}
E_1(t) =&\, e^{(\xi L_S/2v_g)(1+i\alpha)n(t)} E_1(t-\tau_1) \\
&+ K e^{i\Psi_1} e^{(\xi L_S/v_g)(1+i\alpha)n(t)} E_1(t-\tau_{\mathrm{ext}}) \\
&+ T_e e^{i\Pi_1} e^{(\xi L_S/2v_g)(1+i\alpha)n(t)} E_{\mathrm{inj}}^{(1)}
\end{aligned} \tag{1}
$$

$$
\begin{aligned}
E_2(t) =&\, e^{(\xi L_S/2v_g)(1+i\alpha)n(t)} E_2(t-\tau_2) \\
&+ K e^{i\Psi_2} e^{(\xi L_S/v_g)(1+i\alpha)n(t)} E_2(t-\tau_{\mathrm{ext}}) \\
&+ T_e e^{i\Pi_2} e^{(\xi L_S/2v_g)(1+i\alpha)n(t)} E_{\mathrm{inj}}^{(2)}
\end{aligned} \tag{2}
$$

$$
\begin{aligned}
E_f(t) =&\, K_f e^{(1+i\alpha)(\xi L_S/v_g)} \\
&\times \left[E_1(t-\tau_{\mathrm{ext}})e^{i\Psi_{f1}} + E_2(t-\tau_{\mathrm{ext}})e^{i\Psi_{f2}} \right]
\end{aligned} \tag{3}
$$

$$
\begin{aligned}
\frac{dn}{dt} =&\, \frac{I}{q} - \frac{I_{\mathrm{th}}}{q} - \frac{n(t)}{\tau} - \left[\xi n(t) - 2v_g \frac{\ln(|t_r|)}{L_s} \right] \\
&\times \left(|E_1(t)|^2 + |E_2(t)|^2 + |E_f(t)|^2 \right)
\end{aligned} \tag{4}
$$

$$
\Psi_i = \varphi_{\mathrm{ext}} - \frac{2\pi c}{\lambda_i}\tau_{\mathrm{ext}} - 2\varphi_i + \frac{4\pi c}{\lambda_i}\tau_i \quad K = \frac{|t_{\mathrm{ext}}|}{|t_r|^2} \tag{5}
$$

$$
\Psi_{f_i} = \varphi_f - \frac{2\pi c}{\lambda_i}\tau_{\mathrm{ext}} - \varphi_i + \frac{2\pi c}{\lambda_i}\tau_i \quad K_f = \frac{|t_f|}{|t_r|} \tag{6}
$$

$$
\Pi_i = \varphi_e - \frac{2\pi c}{\lambda_i}\tau_i - \varphi_i \quad T_e = \frac{|t_e|}{|t_r|} \tag{7}
$$

$$
E_i(t) = \sqrt{S_i(t)}e^{i\phi_i}. \tag{8}
$$

In (1)–(8), $E_1(t)$ and $E_2(t)$ describe the complex optical field amplitudes in cavity 1 and cavity 2, respectively, $E_f(t)$ is the complex field amplitude for the feedback light, $S_{1,2}(t)$ and $\phi_{1,2}$

are the corresponding photon numbers and phases, ξ is the gain coefficient associated with the linearized SOA gain, α is the linewidth enhancement factor, n is the carrier number of above threshold, L_s is the SOA length, and v_g is the group velocity of the light in the SOA. Furthermore τ is the carrier lifetime, τ_1 and τ_2 are the roundtrip times in cavity 1 and cavity 2, respectively, and τ_{ext} is the roundtrip time through the extended cavity. Moreover, λ_i is the wavelength of the lasing light in each cavity, I is the injection current, I_{th} is the threshold current, and q is the elementary charge unit. Finally, T_e represents the fraction of the external optical field $E_{\mathrm{inj}}^{(i)}$ that is coupled in each cavity, K_f represents the fraction of the lasing light that is fed back into the SOA via the extended cavity, and K is the fraction of the light that is reflected back in the laser via the extended cavity and the SOA facet. The optical phases corresponding to the reflections K_f, K, and T_e in the various cavities are identified with Ψ_{f_i}, Ψ_i, and Π_i, respectively.

By solving (1)–(8), insight can be obtained about bistability in the system described above. Our model accounts for similar physical mechanisms as the model presented in [13]. In that reference, it is shown that depending on the feedback strength, the system can evolve into different stability regimes. The system can evolve into a stable state if a sufficient fraction of the lasing light is fed back into the SOA. With a stable state we mean that the optical field repeats itself after each roundtrip. Our system has two modes of operation that are associated with $E_1(t)$ and $E_2(t)$, respectively. Suppose that both modes could lase, and that the system evolves into the following state:

$$
E_1(t) = E_1(t-\tau_1) \quad E_2(t) = E_2(t-\tau_2). \tag{9}
$$

From substitution of (9) into (1) and (2), we obtain

$$
\begin{aligned}
1 =&\, e^{(\xi L_S/2v_g)(1+i\alpha)n(t)-i\omega_1\tau_1} \\
&+ K e^{i\Psi_1 - i\omega_1\tau_{\mathrm{ext}}} e^{(\xi L_S/v_g)(1+i\alpha)n(t)}
\end{aligned} \tag{10}
$$

$$
\begin{aligned}
1 =&\, e^{(\xi L_S/2v_g)(1+i\alpha)n(t)-i\omega_2\tau_2} \\
&+ K e^{i\Psi_2 - i\omega_2\tau_{\mathrm{ext}}} e^{(\xi L_S/v_g)(1+i\alpha)n(t)}.
\end{aligned} \tag{11}
$$

It follows from (10) and (11) that both roundtrip conditions cannot be simultaneously satisfied, since $\Psi_1 \neq \Psi_2$, $\omega_1 \neq \omega_2$, and both modes share the same laser gain medium (thus, the carrier number n is equal for both lasers). Hence, the phase matching condition can be satisfied by only one of the modes. Therefore, only one mode can lase while the other will be suppressed.

Switching between the states can be realized by injecting external light into the system with a central wavelength equal to that of the suppressed mode. By injection of external light at the wavelength of the suppressed mode, the roundtrip time (1) and (2) can be simultaneously satisfied. Also, the injected light saturates the SOA and, thus, reduces the carrier number n. If the photon number associated with the external light exceeds the threshold value, mode 1 switches off ($E_1(t) = 0$) and mode 2 switches on ($E_2(t) \neq 0$). Hence, the system switches to state 2 in which mode 2 is lasing while mode 1 is suppressed.

The threshold value associated with the number of photons to be injected into the system to switch states can be investigated by using (1)–(8). The parameter values that are used in the

TABLE I
DESCRIPTION OF VALUE OF SYMBOLS USED IN EQUATIONS

| Symbol	Description	Value
τ	Carrier recombination lifetime	$1\ ns$
ξ	Gain coefficient	$3000\ s^{-1}$
v_g	Group velocity in SOA	$8 \times 10^7\ m/s$
α	Linewidth enhancement factor	3
K	Coefficient for the feedback light reflected by the SOA facet	0.01
K_b	Feedback coefficient	0.7
$\tau_{1,2}$	Roundtrip time of cavity 1,2	$7.5 \times 10^{-7}\ s$
τ_{ext}	Feedback time	$10^{-8}\ s$
I	Injection current	$190\ mA$
I_{th}	Threshold current	$172\ mA$
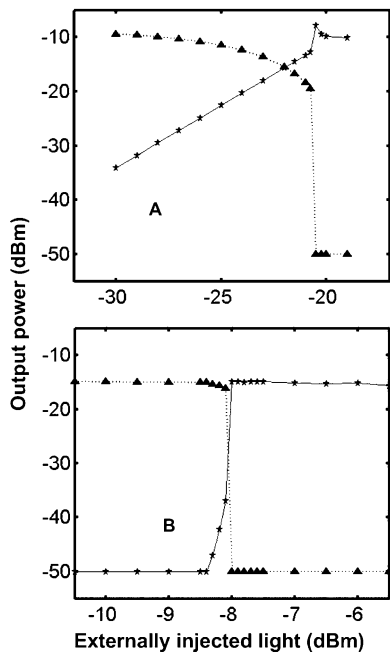
Fig. 2. Output power of both ring lasers versus the optical power of injected light at the wavelength that is initially suppressed. (A) The situation is shown for the case that the injected light copropagates with the lasing light. (B) The situation is shown for the case that the externally injected light counterpropagates with the lasing light.

simulations can be found in Table I. We have investigated the threshold power analytically, but we do not present the result, since the expressions obtained are complicated and offer little insight. It follows, however, that the threshold level can be controlled by the injection current and that the system can change states by using low power optical pulses. Fig. 2(A) shows a simulation result of the optical power in each mode as a function of the externally injected power. The injected light copropagates with the lasing light. It is visible that the system can switch

states if the optical power of the input light is in the order of -20 dBm. This is contrast to the simulation result that is presented in Fig. 2(B), which shows a similar result but now for the case that the injected external light counterpropagates with the lasing light. It follows that the switching power is in the order of -8 dBm. The difference in the switching powers can be explained by the light flows through the SOA. In case of injection of external light that copropagates with the lasing light, the injected light is immediately amplified by the SOA. It follows from Fig. 2(A) that for small injected powers, the injected light is linearly amplified by the SOA. In the case of injection of external light that counterpropagates with the lasing light, the injected light passes one additional time through the SOA before copropagating with the lasing light. Thus, the externally injected light is amplified twice. However, since the reflection on the SOA facet is very small, a very small fraction of the injected light will copropagate with the lasing light and contribute to switching.

III. EXPERIMENT

The schematic of the experimental implementation that has the same conception as the system presented in Fig. 1 is shown in Fig. 3. The flip–flop is realized by using discrete commercially available pigtailed elements that form two unidirectional ring lasers with separate cavities but sharing the same active element. An SOA acts as the laser gain medium. The SOA employed a strained bulk active region. Each cavity contains a Fabry–Pérot filter that acts as a wavelength selective element. The Fabry–Pérot filters have a 3-dB bandwidth of 0.2 nm. A variable attenuator is placed in each ring to control the optical power. Optical isolators are used to allow the light to propagate in only one direction, thus ensuring lasing in one direction. Essential for flip–flop operation is that a fraction of the lasing light is fed back into the laser through an extended cavity. In
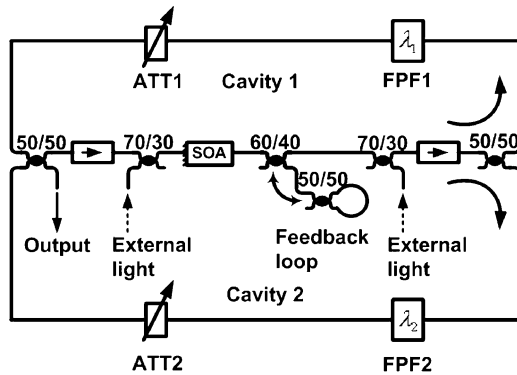
Fig. 3. Experimental implementation of the flip–flop memory. FPF: Fabry–Pérot filter, ATT: attenuator.

Fig. 4. Spectral output of the flip–flop. (A) and (B) show both states in the case that $\lambda_1 = 1550.92$ nm and $\lambda_2 = 1552.52$ nm. The contrast between both states is about 40 dB. (C) and (D) show the case that $\lambda_1 = 1519.34$ nm and $\lambda_2 = 1582.21$ nm indicating that the bistability takes place over a large wavelength range.

this particular configuration, the feedback of lasing light is implemented by using an optical loop mirror made of a 50/50 coupler. The central wavelength λ_1 of the Fabry–Pérot filter in ring cavity 1 is 1550.92 nm and the central wavelength λ_2 of the Fabry–Pérot filter in ring cavity 2 is 1552.52 nm. The system is set in such a way that there are equal optical losses in each cavity. This was realized by setting the attenuator values in ring cavity 1 and ring cavity 2 to 0.5 and 0.82 dB, respectively. Equal optical losses in each cavity imply that both cavities operate at equal threshold current. In our experiments, the SOA injection current is 300 mA and the threshold current is 172 mA. Each cavity contains about 10 m of optical fiber.

In the first experiment, we investigate the bistability of the system by blocking one of the cavities, i.e., cavity 2, and making the system lase in the other cavity, i.e., cavity 1. Unblocking cavity 2 neither prevents cavity 1 from lasing nor leads to lasing in cavity 2. A similar situation takes place the other way around. This is illustrated in Fig. 4(A) and (B), where the optical spectra are shown between the two states after restoration of the cavities. It is visible that the contrast ratio between the lasing state and the suppressed state is 40 dB. The operating wavelength range is also investigated by changing the wavelengths in cavity 1 and cavity 2. It turns out that bistability can be obtained over a large wavelength difference varying from 0.1 nm (limited by the bandwidth of the Fabry–Pérot filter, but not shown in Fig. 4) to 62.87 nm (limited by the optical gain bandwidth of the SOA), as shown in Fig. 4(C) and (D). Moreover, the system is polarization independent; thus, no polarization controlling components are needed in the experimental setup, as shown in Fig. 3.

There are two methods to realize the flip–flop operation. The system is initially lasing at a wavelength λ_1. The first way to change states is to inject external light that counterpropagates with the lasing light with a central wavelength of the suppressed state, i.e., λ_2. This is shown in Fig. 5(A). It turns out that the switching power is -6.63 dBm, when corrected for the splitter loss (70%) of the coupler. After the switching, the system remains lasing at the wavelength λ_2 in spite of the removal of the external light. Note that the trends in the switching curves presented in Fig. 5 are well in agreement with the simulation results presented in Fig. 2. Fig. 5(B) shows a similar result but now in the case of a slightly increased attenuation in the cavities. It follows that in this case the switching power is reduced with 1 dB.
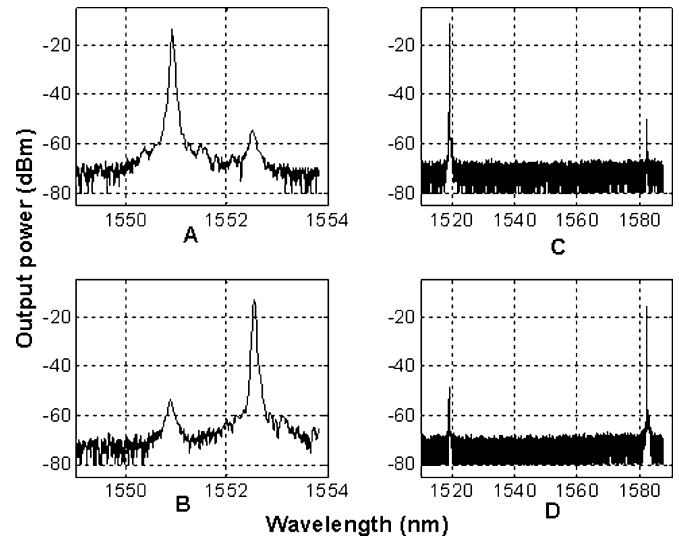
This effect is explained by the fact that a higher attenuation in the cavity leads to a reduced number of photons contribute to the lasing. Hence, switching can be realized by injecting fewer photons in the system. Note that it follows from Fig. 5 that the contrast ratio between the lasing mode and the suppressed mode is less than 40 dB. The reduced contrast ratio is caused by the gain saturation that is introduced by the injected light.

The second way to change states is to inject external light that copropagates with the lasing light with a central wavelength of the suppressed state. The result is shown in Fig. 5(C). In this case, the switching power is reduced to -19.02 dBm. Note that the simulation result presented in Fig. 2 is well in agreement with the experimental result. Fig. 5(D) shows the case in which the attenuation in the cavity is enlarged. Similarly as in the case presented in Fig. 5(B), it is visible that the injected switching power reduces. It has to be remarked that the transition regime (as indicated in Fig. 5) is not stable. This implies that switching is only guaranteed if the injected power exceeds the transition regime. We did not observe a hysteresis effect in the switching.

The switching speed of the flip–flop memory was investigated experimentally and numerically. Numerical results indicate that it takes approximately 30 round-trip times to switch the flip–flop state. This was confirmed by experiments. Decreasing the cavity length is essential to realize higher switching speeds. The system presented in this paper was made out of commercially available fiber pigtailed components, which made that the total cavity length was in the order of 10 m. It should be remarked that this concept allows photonic integration, which implies that the cavity length should be reduced to a few millimeters. Simulation results indicate that our results still hold for photonic integrated systems. Also, the roundtrip-time equations that are used in this paper could be easily reformulated as rate equations that well describe the behavior of an integrated flip–flop memory.
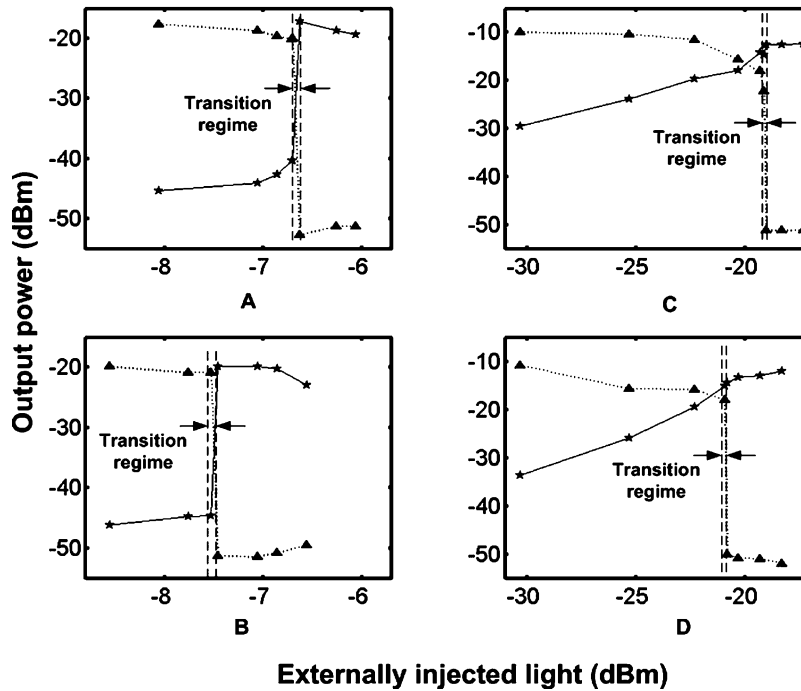
Externally injected light (dBm)

Fig. 5.   Flip–flop output power versus the power of the externally injected light. The SOA parameters can be found in Table I; furthermore, $\lambda_1 = 1550.92$ nm and $\lambda_2 = 1552.52$ nm. The wavelength of the injected light is 1552.52 nm. (A) and (C) show the results for front and back injection of external light if the attenuator values were 0.50 dB (for attenuator 1) and 0.82 dB (for attenuator 2). (B) and (D) show similar results, but now for the attenuation values of 1.00 dB (attenuator 1) and 1.32 dB (attenuator 2).

IV. CONCLUSION

In this paper, we present an optical flip–flop based on two coupled ring lasers that share a SOA which acts as the laser gain medium. Essential for the flip–flop operation is the presence of optical feedback. The bistability is caused by that the feedback of the lasing light, which makes that the phase matching condition in only one of the lasers can be satisfied. We have presented numerical and experimental results that are in agreement with each other. The experimental setup was realized by using commercially available fiber pigtailed components. We have observed a 40-dB contrast ratio between both states. The switching power was -19.02 dBm if the switching light is injected in the same direction as the lasing light and -6.63 dBm if the light was injected in the opposite direction. Moreover, the system is polarization independent.

In the flip–flop implementation as presented in this paper, we did not succeed to demonstrate narrow linewidth operation. This might be due to the bandwidth of the filters (0.2 nm) used in the experiment in combination with the large cavity length (10 m). In [13], the dynamics of a semiconductor laser with feedback is investigated. It was observed in [13] that in such a system instabilities due to coherence collapse can take place. We did not observe hopping between modes located around different bands even if the bands were separated at a spectral distance of 0.1 nm. A possible way to prevent these instabilities could be by either increasing the amount of feedback or by making the feedback very small [13].

The main advantage of this concept is, however, the fact that this concept could be easily extended. The mathematical formulation reveals that multistable behavior is possible if the number of cavities is increased. A multiple-state optical flip–flop memory forms an important building block for multiple-state all-optical packet switches that operate at low power.

APPENDIX

In Fig. 1 a schematic of our flip–flop configuration is given. The roundtrip equations associated with the system are

$$
\begin{aligned}
E_1(t) = {} & t_1 e^{-ik_s L_s} e^{-i\omega_1 \tau_1} E_1(t - \tau_1) \\
& + t_{\text{ext}} E_1(t - \tau_{\text{ext}}) e^{-2ik_s L_s} e^{-i\omega_1 \tau_{\text{ext}}} \\
& + t_e E_{\text{inj}}^{(1)} e^{-ik_s L_s}
\end{aligned}
\tag{A.1}
$$

$$
\begin{aligned}
E_2(t) = {} & t_2 e^{-ik_s L_s} e^{-i\omega_2 \tau_2} E_2(t - \tau_2) \\
& + t_{\text{ext}} E_2(t - \tau_{\text{ext}}) e^{-2ik_s L_s} e^{-i\omega_2 \tau_{\text{ext}}} \\
& + t_e E_{\text{inj}}^{(2)} e^{-ik_s L_s}
\end{aligned}
\tag{A.2}
$$

and

$$
\begin{aligned}
E_f(t) = t_f \Big\lfloor & E_1(t - \tau_{\text{ext}}) e^{-ik_s L_s} e^{-i\omega_1 \tau_{\text{ext}}} \\
& + E_2(t - \tau_{\text{ext}}) e^{-ik_s L_s} e^{-i\omega_2 \tau_{\text{ext}}} \Big\rfloor
\end{aligned}
\tag{A.3}
$$

where

$$
t_1 = r_a r_b r_c r_d \sqrt{1 - t_e^2} \quad t_2 = r_a r_b t_c t_d \sqrt{1 - t_e^2}
\tag{A.4}
$$

and

$$
t_{\text{ext}} = t_b^2 r_s r_{\text{ext}} \quad t_f = t_b^2 r_{\text{ext}}.
\tag{A.5}
$$

In (A.1)–(A.5), $E_1(t)$ and $E_2(t)$ are the complex optical field amplitudes in cavity 1 and cavity 2, respectively, $E_f(t)$ is the complex field amplitude of the light that is fed back into the SOA in the counterpropagating direction, r_i and $t_i (i \in \{a, b, c, d, e\})$

are the reflections and transmissions through the beam splitters in the system, r_{ext} is the reflectivity of the end mirror in the feedback loop, r_s is the reflectivity of SOA facet, τ_1 and τ_2 are the roundtrip times in cavity 1 and cavity 2, respectively, and τ_{ext} is the roundtrip time through the feedback loop. The SOA length is represented by L_s, ω_1 and ω_2 are the central optical frequencies of the lasing light in cavity 1 and cavity 2, respectively, k_s is the wave number of the light propagating through the SOA, and $E_{\text{inj}}^{(1)}$ and $E_{\text{inj}}^{(2)}$ represent the optical field associated with the externally injected light. In the roundtrip equations as given above, it is assumed that the amplification of the light propagating through the SOA is wavelength independent. Also, it is assumed that the central wavelength of $E_{\text{inj}}^{(1)}$ is equal to that of $E_1(t)$ and that the central wavelength of $E_{\text{inj}}^{(2)}$ is equal to that of $E_2(t)$. If we introduce the notation $t_1 = |t_1|e^{i\varphi_1}$, $t_2 = |t_2|e^{i\varphi_2}$, $t_{\text{ext}} = |t_{\text{ext}}|e^{i\varphi_{\text{ext}}}$, $t_f = |t_f|e^{i\varphi_f}$ and $t_e = |t_e|e^{i\varphi_e}$, it is found that (A.1) and (A.3) are equivalent with

$$
\begin{aligned}
E_1(t) = &|t_1|e^{-ik_sL_s}e^{-i\omega_1\tau_1}e^{i\varphi_1}E_1(t-\tau_1) \\
&+ |t_{\text{ext}}|E_1(t-\tau_{\text{ext}})e^{-2ik_sL_s}e^{-i\omega_1\tau_{\text{ext}}}e^{i\varphi_{\text{ext}}} \\
&+ |t_e|E_{\text{inj}}^{(1)}e^{-ik_sL_s}e^{i\varphi_e}
\end{aligned}
\tag{A.6}
$$

$$
\begin{aligned}
E_2(t) = &|t_2|e^{-ik_sL_s}e^{-i\omega_2\tau_2}e^{i\varphi_2}E_2(t-\tau_2) \\
&+ |t_{\text{ext}}|E_2(t-\tau_{\text{ext}})e^{-2ik_sL_s}e^{-i\omega_2\tau_{\text{ext}}}e^{i\varphi_{\text{ext}}} \\
&+ |t_e|E_{\text{inj}}^{(2)}e^{-ik_sL_s}e^{i\varphi_e}
\end{aligned}
\tag{A.7}
$$

$$
\begin{aligned}
E_f(t) = |t_f|e^{i\varphi_f}\big[&E_1(t-\tau_{\text{ext}})e^{-ik_sL_s}e^{-i\omega_1\tau_{\text{ext}}} \\
&+ E_2(t-\tau_{\text{ext}})e^{-ik_sL_s}e^{-i\omega_2\tau_{\text{ext}}}\big].
\end{aligned}
\tag{A.8}
$$

We define the SOA gain by using that

$$
\frac{dE}{dz} = [G_R(N) + iG_I(N)]E
\tag{A.9}
$$

where the real and imaginary parts of the gain account for the confinement. If we integrate (A.9) over a SOA length, we obtain

$$
E(L_s) = e^{[G_R(N)L_s + iG_I(N)L_s]} \equiv e^{-ikL_s}.
\tag{A.10}
$$

If we furthermore linearize the real and imaginary parts of the complex gain around the threshold value N_{th}, we find

$$
G_R(N) = G_R(N_{\text{th}}) + \frac{\xi}{2v_g}(N - N_{\text{th}})
\tag{A.11}
$$

$$
G_I(N) = G_I(N_{\text{th}}) + \frac{\xi\alpha}{2v_g}(N - N_{\text{th}})
\tag{A.12}
$$

where ξ is the linearized gain coefficient, v_g the group velocity, and α the linewidth enhancement factor. If we substitute (A.10)–(A.12) into (A.6)–(A.8), we find

$$
\begin{aligned}
E_1(t) = &e^{(1+i\alpha)(\xi L_S/2v_g)n(t)}E_1(t-\tau_1) \\
&+ \frac{|t_{\text{ext}}|}{|t_r|^2}e^{i[\varphi_{\text{ext}}-\omega_0\tau_{\text{ext}}+2G_I(N_{\text{th}})L_S]} \\
&\times e^{(1+i\alpha)(\xi L_S/v_g)n(t)}E_1(t-\tau_{\text{ext}}) \\
&+ \frac{|t_e|}{|t_r|}e^{i[\varphi_e+G_I(N_{\text{th}})L_S]} \\
&\times e^{(1+i\alpha)(\xi L_S/2v_g)n(t)}E_{\text{inj}}^{(1)}
\end{aligned}
\tag{A.13}
$$

$$
\begin{aligned}
E_2(t) = &e^{(1+i\alpha)(\xi L_S/2v_g)n(t)}E_2(t-\tau_2) \\
&+ \frac{|t_{\text{ext}}|}{|t_r|^2}e^{i[\varphi_{\text{ext}}-\omega_0\tau_{\text{ext}}+2G_I(N_{\text{th}})L_S]} \\
&\times e^{(1+i\alpha)(\xi L_S/v_g)n(t)}E_2(t-\tau_{\text{ext}}) \\
&+ \frac{|t_e|}{|t_r|}e^{i[\varphi_e+G_I(N_{\text{th}})L_S]} \\
&\times e^{(1+i\alpha)(\xi L_S/2v_g)n(t)}E_{\text{inj}}^{(2)}
\end{aligned}
\tag{A.14}
$$

$$
\begin{aligned}
E_f(t) = &\frac{|t_f|}{|t_r|}e^{(1+i\alpha)(\xi L_s/2v_g)} \\
&\times \Big[E_1(t-\tau_{\text{ext}})e^{i[\varphi_f-\omega_1\tau_{\text{ext}}+G_I(N_{\text{th}})L_S]} \\
&\quad + E_2(t-\tau_{\text{ext}}) \\
&\qquad \times e^{i[\varphi_f-\omega_2\tau_{\text{ext}}+G_I(N_{\text{th}})L_S]}\Big]
\end{aligned}
\tag{A.15}
$$

where it was used that $n = N - N_{\text{th}}$ and that the following roundtrip condition has to be satisfied:

$$
\varphi_i - \omega_i\tau_i + G_I(N_{\text{th}})L_s = 2n\pi \quad e^{G_R(N_{\text{th}})L_S} = \frac{1}{|t_r|}.
\tag{A.16}
$$

In (A.16), it was assumed that each cavity satisfies the same roundtrip condition ($|t_1| = |t_2| = |t_r|$). We can further simplify (A.13)–(A.15) by introducing the following notation:

$$
\Psi_i = \varphi_{\text{ext}} - \frac{2\pi c}{\lambda_i}\tau_{\text{ext}} - 2\varphi_i + \frac{4\pi c}{\lambda_i}\tau_i
$$

$$
K = \frac{|t_{\text{ext}}|}{|t_r|^2}
\tag{A.17}
$$

$$
\Psi_{f_i} = \varphi_f - \frac{2\pi c}{\lambda_i}\tau_{\text{ext}} - \varphi_i + \frac{2\pi c}{\lambda_i}\tau_i
$$

$$
K_f = \frac{|t_f|}{|t_r|}
\tag{A.18}
$$

$$
\Pi_i = \varphi_e - \frac{2\pi c}{\lambda_i}\tau_i - \varphi_i
$$

$$
T_e = \frac{|t_e|}{|t_r|}
\tag{A.19}
$$

where it was used that $\omega_i = (2\pi c/\lambda_i)$. If (A.17)–(A.19) are substituted in (A.13)–(A.15), we find

$$
\begin{aligned}
E_1(t) = &e^{(\xi L_S/2v_g)(1+i\alpha)n(t)}E_1(t-\tau_1) \\
&+ Ke^{i\Psi_1}e^{(\xi L_S/v_g)(1+i\alpha)n(t)}E_1(t-\tau_{\text{ext}}) \\
&+ T_ee^{i\Pi_1}e^{(\xi L_S/2v_g)(1+i\alpha)n(t)}E_{\text{inj}}^{(1)}
\end{aligned}
\tag{A.20}
$$

$$
\begin{aligned}
E_2(t) = &e^{(\xi L_S/2v_g)(1+i\alpha)n(t)}E_2(t-\tau_2) \\
&+ Ke^{i\Psi_2}e^{(\xi L_S/v_g)(1+i\alpha)n(t)}E_2(t-\tau_{\text{ext}}) \\
&+ T_ee^{i\Pi_2}e^{(\xi L_S/2v_g)(1+i\alpha)n(t)}E_{\text{inj}}^{(2)}
\end{aligned}
\tag{A.21}
$$

$$
\begin{aligned}
E_f(t) = &K_fe^{(1+i\alpha)(\xi L_s/2v_g)} \\
&\times \big[E_1(t-\tau_{\text{ext}})e^{i\Psi_{f_1}} + E_2(t-\tau_{\text{ext}})e^{i\Psi_{f_2}}\big].
\end{aligned}
\tag{A.22}
$$

Finally, the rate equation for the carrier number is

$$
\begin{aligned}
\frac{dn}{dt} = &\frac{I}{q} - \frac{I_{\text{th}}}{q} - \frac{n(t)}{\tau} \\
&- 2v_gG_R(n)\left(|E_1(t)|^2 + |E_2(t)|^2 + |E_f(t)|^2\right)
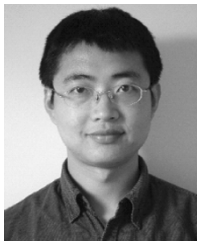\end{aligned}
\tag{A.23}
$$

where I represents the injection current and q is the elementary charge unit. By using (A.11) and (A.16), we find that (A.23) is equivalent with

$$\frac{dn}{dt} = \frac{I}{q} - \frac{I_{th}}{q} - \frac{n(t)}{\tau} - \left[\xi n(t) - 2v_g \frac{\ln(|t_r|)}{L_s}\right]$$
$$\times \left(|E_1(t)|^2 + |E_2(t)|^2 + |E_f(t)|^2\right). \quad \text{(A.24)}$$

Equations (A.20)–(A.22) in combination with (A.24) describe the system presented in Fig. 1.

Yong Liu was born in China in 1970. He received the M.S. degree in electronic engineering from the University of Electronic Science and Technology of China, Chengdu, in 1994. He is currently working toward the Ph.D. degree at Eindhoven University of Technology, Eindhoven, The Netherlands.

From 1994 to 2000, he worked at the University of Electronic Science and Technology of China in teaching and research. His research interest is all-optical buffering by using all optical signal processing.

REFERENCES

[1] M. T. Hill, A. Srivatsa, N. Calabretta, Y. Liu, H. de Waardt, G. D. Khoe, and H. J. S. Dorren, "1 × 2 optical packet switch using all-optical header processing," *Electron. Lett.*, vol. 37, pp. 774–775, 2001.

[2] H. Kawaguchi, *Bistabilities and Nonlinearities in Laser Diodes*. Boston, MA: Artech House, 1994.

[3] M. Takenaka and Y. Nakano, "Multimode interference bistable laser diode," *IEEE Photon. Technol. Lett.*, vol. 15, pp. 1035–1037, Aug. 2003.

[4] ——, "Realization of all-optical flip–flop using bistable laser diode with nonlinear directional coupler," *IEEE Photon. Technol. Lett.*, vol. 16, 2004, to be published.

[5] L. Xu, C. Wang, V. Baby, I. Glesk, and P. R. Prucnal, "Optical spectrum bistability in a semiconductor fiber ring laser through gain saturation in a SOA," *IEEE Photon. Technol. Lett.*, vol. 14, pp. 149–151, Feb. 2002.

[6] B. C. Wang, L. Xu, V. Baby, I. Glesk, and P. R. Prucnal, "State selection of a bistable SOA ring laser for bit-level optical memory applications," *IEEE Photon. Technol. Lett.*, vol. 14, pp. 989–991, 2002.

[7] M. T. Hill, H. de Waardt, G. D. Khoe, and H. J. S. Dorren, "All-optical flip–flop based on coupled laser diodes," *IEEE J. Quantum Electron.*, vol. 37, pp. 405–413, Mar. 2001.

[8] ——, "Fast optical flip–flop by use of Mach–Zehnder interferometers," *Microwave Opt. Technol. Lett.*, vol. 31, pp. 411–415, 2001.

[9] Y. Liu, M. T. Hill, H. de Waardt, G. D. Khoe, D. Lenstra, and H. J. S. Dorren, "All-optical flip–flop memory based on two coupled polarization switches," *Electron. Lett.*, vol. 38, pp. 904–906, 2002.

[10] H. J. S. Dorren, M. T. Hill, Y. Liu, N. Calabretta, A. Srivatsa, F. M. Huijskens, H. de Waardt, and G. D. Khoe, "Optical packet switching and buffering by using all-optical signal processing methods," *J. Lightwave Technol.*, vol. 21, pp. 2–12, Jan. 2003.

[11] J. J. Liang, S. T. Lau, M. H. Leary, and J. M. Ballantyne, "Unidirectional operation of waveguide diode ring lasers," *Appl. Phys. Lett.*, vol. 70, pp. 1192–1194, 1997.

[12] J. P. Hohimer, G. A. Vawter, and D. C. Craft, "Unidirectional operation in a semiconductor ring diode laser," *Appl. Phys. Lett.*, vol. 62, pp. 1185–1187, 1993.

[13] N. Schunk and K. Petermann, "Numerical analysis of the feedback regimes for a single-mode semiconductor laser with external feedback," *IEEE J. Quantum Electron.*, vol. 24, pp. 1242–1247, July 1988.

Daan Lenstra was born in Amsterdam, The Netherlands, in 1947. He received the M.Sc. degree in theoretical physics from the University of Groningen, Groningen, The Netherlands, and the Ph.D. degree from Delft University of Technology, Delft, The Netherlands. His thesis work was on polarization effects in gas lasers.

Since 1979, he researched topics in quantum electronics, laser physics, and condensed matter physics. In 1991, he joined the Vrije Universiteit, Amsterdam, holding a chair in theoretical quantum electronics. In 2000, he also became a part-time Professor at the Department of Electrical Engineering, Eindhoven University of Technology, Eindhoven, The Netherlands, where since 2002 he has occupied a chair on ultrafast photonics as part-time (0.4) Professor. He has (co)authored more than 200 publications in international scientific journals and (co)edited six books and several special journal issues. His research interests are nonlinear and ultrafast dynamics of semiconductor optical amplifiers and diode lasers, quantum optics in small semiconductor structures, and near-field optics.

Dr. Lenstra is a Member of the IEEE Laser and Electro-Optics Society (LEOS), the Optical Society of America (OSA) and the European Physical Society (EPS) and acts regularly as program (co)chair for international meetings.

Martin T. Hill was born in Sydney, Australia, in 1968. He received the B.E. degree (with first-class honors) and the M.Eng.Sc. degree from the University of Western Australia, Adelaide, in 1990 and 1992, respectively, and the Ph.D degree in 1997 from Curtin University of Technology, Perth, W. Aust., Australia.

During 1990, he was a Member of Technical Staff at QPSX Communications Pty. Ltd., and from 1993 to 1998, he worked at the Australian Telecommunications Research Institute. Since 1998, he has been working in the Department of Electrical Engineering, Technical University of Eindhoven, Eindhoven, The Netherlands, where he is involved in research on photonic components for optical packet switching.

Shaoxian Zhang was born in Liaoning, China, in 1977. He received the M.Sc. degree in optical engineering from the University of Electronic Science and Technology of China, Chengdu, in 2002. He is currently working toward the Ph.D. degree at Eindhoven University of Technology, Eindhoven, The Netherlands.

His research interest is optical memory.

Heongkyu Ju was born in Seoul, Korea, in 1970. He received the B.S. degree in physics and the M.Sc. degree in quantum field theory of elementary particle physics from the Korea University, Seoul, Korea, in 1993 and 1998, respectively, and the Ph.D. degree in condensed matter physics at the University of Oxford, Oxford, U.K. in 2003.

He is currently a Postdoctoral Researcher in the Electro-optical Communication Group, Eindhoven University of Technology, Eindhoven, The Netherlands. His research interests include ultrafast all-optical switching and memories by using nonlinear ultrafast carrier dynamics in semiconductor optical amplifiers.

Giok-Djan Khoe (S'71–M'71–SM'85–F'91) was born in Magelang, Indonesia, in 1946. He received the Elektrotechnisch Ingenieur degree (*cum laude*) from the Eindhoven University of Technology, Eindhoven, The Netherlands, in 1971.

He was a Researcher with the Dutch Foundation for Fundamental Research on Matter (FOM), Laboratory on Plasma Physics, Rijnhuizen, The Netherlands. In 1973, he moved to the Philips Research Laboratories to begin research in the area of optical fiber communication systems. In 1983, he was appointed part-time Professor at Eindhoven University of Technology, becoming a full Professor in 1994. Currently, he is Chairman of the Department of Telecommunication Technology and Electromagnetics (TTE). Most of his work has been devoted to single-mode fiber systems and components. His research programs are centered on ultrafast all-optical signal processing, high-capacity transport systems, and systems in the environment of the users. He has more than 40 U.S. patents and has authored and coauthored more than 100 papers, invited papers, and book chapters. In Europe, he is closely involved in Research Programs of the European Community and in Dutch national research programs, as a participant, evaluator, auditor, and program committee member. He is one of the founders of the Dutch COBRA University Research Institute. In 2001, he brought four groups together to start a new international alliance called the European Institute on Telecommunication Technologies (eiTT).

Dr. Khoe is an Associate Editor of the IEEE JOURNAL OF QUANTUM ELECTRONICS and the appointed President of the IEEE Lasers and Electro-Optics Society (LEOS). Recently, he was General Cochair of the ECOC 2001. He has served the IEEE LEOS organization as a European Representative in the BoG, a Vice President of Finance and Administration, a BoG Elected Member, and a member of the Executive Committee of the IEEE Benelux Section, and was Founder of the LEOS Benelux Chapter. He is the current Junior Past President of LEOS. He received the MOC/GRIN Award in 1997 and was a recipient of the prestigious "Top Research Institute Photonics" grant that is awarded to COBRA in 1998 by the Netherlands Ministry of Education, Culture and Science.

H. J. S. Dorren received the M.Sc. degree in theoretical physics and the Ph.D. degree from Utrecht University, Utrecht, The Netherlands, in 1991 and 1995, respectively.

After a postdoctoral position, he joined Eindhoven University of Technology, Eindhoven, The Netherlands, in 1996, where he currently serves as an Associate Professor. In 2002 he was also a Visiting Researcher at the National Institute of Industrial Science and Technology (AIST), Tsukuba, Japan. His research interests include optical packet switching, digital optical signal processing, and ultrafast photonics.